Short communication

A reinvestigation of EXAFS and EPR spectroscopic measurements of chromium(VI) reduction by coir pith

Parinda Suksabye [a], Niramon Worasith [b], Paitip Thiravetyan [b], Akira Nakajima [c], Bernard A. Goodman [d],*

[a] Department of Environmental Science, Faculty of Science and Technology, Suan Dusit Rajabhat University, 10300, Thailand
[b] Division of Biotechnology, School of Bioresources and Technology King Mongkut's University of Technology, Thonburi, Bangkhuntien, Bangkok, Thailand
[c] Division of Chemistry, Department of Medical Science, Faculty of Medicine, University of Miyazaki, Kiyotake, Miyazaki 8891692, Japan
[d] Health and Environment Department, Unit of Environmental Resources & Technologies, Austrian Institute of Technology, Seibersdorf A-2444, Austria

ARTICLE INFO

ABSTRACT

New measurements using extended X-ray absorption fine structure (EXAFS) and electron paramagnetic resonance (EPR) techniques are consistent with Cr in the Cr(III) oxidation state as the main product from the adsorption of Cr(VI) on coir pith. These confirm the previous X-ray measurements, but differ from the results of previous EPR studies, which indicated that Cr(V) was the main form of Cr. The reason for this discrepancy is the presence of a broad signal from Cr(III) in an unsymmetrical environment that was missed previously; the Cr(V) component is in fact only a minor reaction product. As a result of this problem with spectral acquisition and interpretation, some simple recommendations are presented for conducting EPR investigations on natural systems.

© 2010 Published by Elsevier B.V.

1. Introduction

The production of low cost adsorbents for the clean-up of contaminated waters is of considerable importance for the improvement of environmental quality in developing countries. One product that is currently showing potential for use in the removal of environmental pollutants is coir pith, an agro-industrial waste product that is derived from coconut husk. Examples have been published recently demonstrating the use of coir pith in its natural form [1–5] or after chemical modification to improve its adsorption capacity or specificity [4,6–9].

In previous studies, the mechanisms of Cr(VI) adsorption by coir pith were investigated [2,3,5], and the adsorbed species characterized by X-ray absorption near edge structure (XANES) [2] and electron paramagnetic resonance (EPR) spectroscopy [3,5]. Although both spectroscopic techniques indicated that Cr(VI) adsorption involved reduction of Cr(VI) to lower oxidation states, there were fundamental differences in the conclusions as to the identities of the final forms of the metal. The most intense signal that was seen in the EPR spectra was associated with Cr(V), whereas XANES spectra indicated that Cr(III) was the major form of the metal, and no evidence was observed for the presence of Cr(V) [2].

Furthermore, desorption studies [5] indicated that Cr(III) accounted for ~75% of the Cr adsorbed on coir pith, although these results suggested that some Cr(V) and Cr(VI) forms were also present.

In order to address the discrepancy in the conclusions from these reports, further measurements have now been performed using the EXAFS (extended X-ray absorption fine structure) and EPR techniques, and these are reported in the present communication.

2. Materials and methods

$Na[Cr(O)(ehba)_2]\cdot H_2O$ and the products of Cr(VI) adsorption on coir pith at pH 2 and 10 were described by Suksabye et al. [5]. Coir pith (<75 μm) was treated with Cr(VI) solution (2%, w/v) at pH 2 or 10 for 18 h, then dried for 1 h at 105 °C, and ground with an agate mortar before use for the spectroscopic measurements. Additional samples were prepared using mixed Cr(VI)/Al(III) solutions with Cr:Al ratios between 1:1 and 1:10. Cr_2O_3 enriched to >99% in the ^{53}Cr isotope was obtained from AERE, Harwell, UK. This was dissolved in strong alkali, precipitated as $[Cr(OH)_6]^{3-}$, then redissolved in distilled water and oxidized to Cr(VI) using H_2O_2. The preparation of ^{53}Cr/coir pith was performed as described above for the natural abundance isotopes.

For EXAFS measurements, samples were loaded into sample plates and secured with kapton tape for analysis at the National Synchrotron Research Center, Thailand on beamline 8. Transmission XAS data for Cr were collected with K edges and an energy of

* Corresponding author. Tel.: +43 50550 3434; fax: +43 50550 3520.
E-mail address: bernard_a_goodman@yahoo.com (B.A. Goodman).

5.989 keV using an InSb(111) crystal monochromator. The beam-line was operated with an energy of 1.2 GeV and current in the range 27–50 mA. $K_2Cr_2O_7$, $Na[Cr(O)(ehba)_2]\cdot H_2O$ and $Cr_2(SO_4)_3\cdot xH_2O$ were used as standards for Cr(VI), Cr(V) and Cr(III), respectively.

For data analysis, pre-edge subtraction and normalization of the experimental spectra was performed using the ATHENA program [10], then the post-edge background was removed with the program AUTOBK [11]. Curve fitting was performed using the EXCURV98 software [12]. The EXAFS energy spectra were converted to k space (wave vector space, $Å^{-1}$), and the scattering curve was weighted by k^3 to enhance damped scattering oscillations, before Fourier transformation to yield interatomic distances. The number of atoms coordinated to the absorbing atom and the Debye–Waller factors (σ^2) were ascertained by least squares fits of Fourier transformed EXAFS data.

All of the EPR spectra were recorded at X-band frequencies on CW spectrometers using Gunn diodes as the microwave source. Most of the spectra were acquired on a Bruker EMX spectrometer equipped with a high sensitivity cavity, but some were obtained using a JEOL (JES-RE2X) spectrometer; in all cases a modulation frequency of 100 kHz was used. Other conditions used for spectral acquisition are presented in the relevant figure captions. g-values are expressed relative to solid DPPH ($g = 2.0036$), which was used as an external standard.

3. Theory

In order to appreciate the significance of the various spectroscopic measurements, the types of results that can be obtained from the EXAFS and EPR techniques will first of all be considered briefly for the Cr(VI), Cr(V) and Cr(III) oxidation states which have $3d^0$, $3d^1$, and $3d^3$ electronic configurations, respectively [13].

EXAFS patterns are determined by the coordination environment of a metal, and are fitted to models that reflect the number, chemical nature and distances to the elements in the coordination shell, i.e. the nearest neighbor atoms. Since the bond length is directly related to the metal charge, EXAFS is very sensitive to metal ion oxidation states. For example, the Cr–O bond distances increase progressively from Cr(VI) to Cr(V) to Cr(III); values for the $K_2Cr_2O_7$ [14], $Na[Cr(O)(ehba)_2]\cdot H_2O$, and chromium(III) sulfate or nitrate [15] being 1.64 Å, 1.88 Å and 1.95 Å, respectively.

EPR spectroscopy is only able to provide information on chromium in the Cr(V) and Cr(III) oxidation states; it gives no information on Cr(VI) ions, which are diamagnetic. Oxochromium(V) compounds are the main forms of Cr(V). They have axial symmetry as a result of the Cr–O bond and this results in stabilization of the d_{xy} (or $d_{x^2-y^2}$) orbital. EPR spectra are to a first approximation characterized by g-values given by the following relationships:

$$g_{xx} = 2.0023 - \frac{2\alpha^2\gamma_2^2\xi}{\Delta(d_{xy} - d_{xz})}$$

$$g_{yy} = 2.0023 - \frac{2\alpha^2\gamma_1^2\xi}{\Delta(d_{xy} - d_{yz})}$$

$$g_{zz} = 2.0023 - \frac{8\alpha^2\beta^2\xi}{\Delta(d_{xy} - d_{x^2-y^2})}$$

where α, β, γ_1, and γ_2 are the molecular orbital coefficients of the d_{xy}, $d_{x^2-y^2}$, d_{xz} and d_{yz} orbitals, respectively, ξ is the single electron spin–orbit coupling constant, and the Δ values correspond to the energy separations between the designated 3d-orbitals. In axial symmetry, $\Delta(d_{xy} - d_{xz}) = \Delta(d_{xy} - d_{yz})$ and $g_{xx} = g_{yy}$; these g-values are commonly known as $g_\perp$, with g_{zz} called $g_{||}$, since these g-values respectively correspond to the magnetic field lying perpendicular
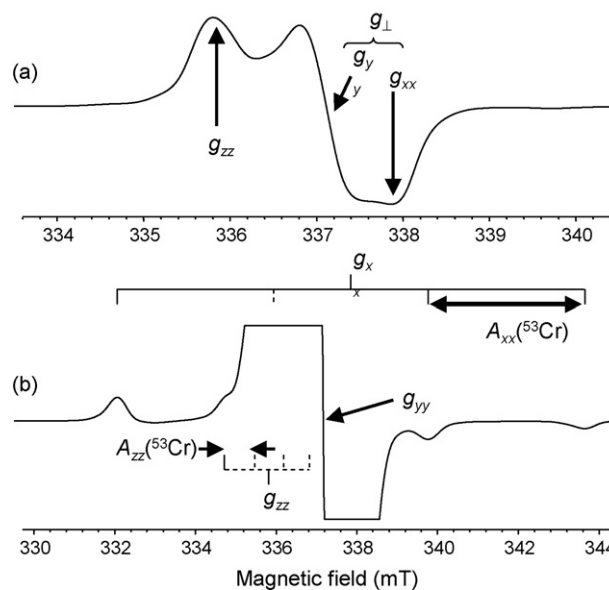

Fig. 1. EPR spectrum of a solution of $[Cr(O)(ehba)_2]^-$ in methanol at 77 K, (a) showing the origin of the g-values, (b) the ^{53}Cr hyperfine structure, that can be resolved at high instrument gain. Spectra were recorded using 0.2 mW microwave power and 0.5 mT modulation amplitude.

and parallel to the principal axis of the molecular orbital containing the unpaired electron. Although $g_\perp$ and $g_{||}$ are both usually <2 for Cr(V), their relative magnitudes are dependent on the bonding characteristics of the molecule under investigation.

The EPR spectrum of $Na[Cr(O)(ehba)_2]\cdot H_2O$ in methanol solution at 77 K (Fig. 1a) is an example of a rigid limit spectrum for isolated Cr(V) complexes. Three g-values are resolved with $g_{zz} = 1.9855$, $g_{yy} = 1.9777$ and $g_{xx} = 1.9734$, the small difference between the g_{xx} and g_{yy} values indicate some deviation from axial symmetry in this complex. With an unknown sample, it would not have been possible to distinguish between this situation and the presence of more than one Cr(V) species with axial symmetry, so caution must always be exercised when interpreting such EPR spectra from natural samples.

Natural chromium also contains of >1 isotope, although ^{53}Cr is the only one with non-zero spin, I. For ^{53}Cr the natural abundance is 9.5% and $I = 3/2$, so each EPR spectrum contains four ($2I + 1$) component lines (hyperfine structure (hfs) designated by A), each with intensity $\sim$2.5% of the main spectrum as a result of the interaction of the unpaired electron with ^{53}Cr. In samples of environmental origin, where other paramagnetic components may be present, the observation of hfs from ^{53}Cr provides unambiguous identification of Cr as the source of an EPR signal. The magnitudes of the A-values provide information on the molecular orbital coefficients, and are complementary to the g-values in characterizing the electronic properties of the ion (e.g. [16]). This is illustrated in Fig. 1b. The analysis of this spectrum is actually quite complex. Three ^{53}Cr satellite peaks associated with g_{xx} are clearly resolved and correspond to an $A_{xx}(^{53}Cr)$ value of 3.87 mT. However, only one other peak attributable to ^{53}Cr is resolved. This must be the low field peak associated with g_{zz}, and hence corresponds to an $A_{zz}(^{53}Cr)$ of 0.71 mT; if it were associated with g_{yy}, it would correspond to a hyperfine coupling constant of 1.61 mT, but there is no corresponding peak on the high field side of the main ^{52}Cr resonance. In fact no ^{53}Cr peaks associated with g_{yy} are resolved, but their positions can be estimated by using the relationship $A_{iso} = (A_{xx} + A_{yy} + A_{zz})/3$, where A_{iso} is the isotropic hyperfine splitting observed in fluid solution. Fluid solution measurements (not shown) gave $g_{iso} = 1.9783$ and $A_{iso} = 1.82$ mT, and hence a value of 0.88 mT would be expected
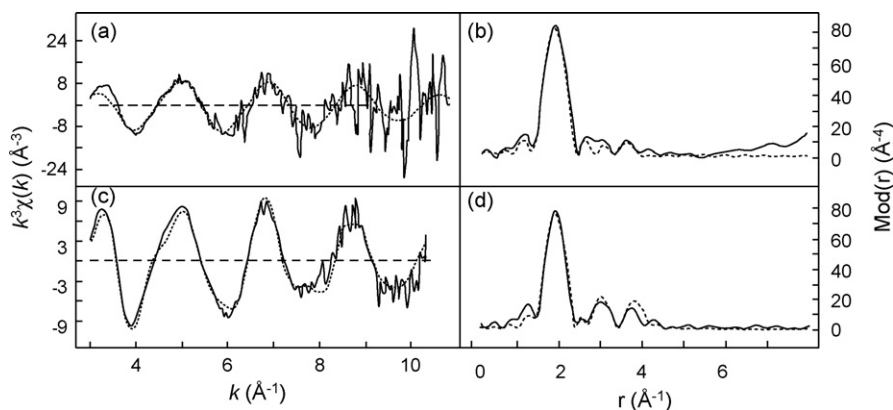
Fig. 2. Experimental (solid lines) and fitted (dashed lines) k^3-weighted EXAFS spectra (a, c) and their Fourier transforms (b, d) of Cr(VI) adsorbed on coir pith (a, b), and chromium(III) sulfate hydrate ($Cr_2(SO_4)_3 \cdot xH_2O$) (c, d).

for $A_{yy}(^{53}Cr)$. This is in fact a maximum value for A_{yy}, since a smaller value would occur if the g- and A-tensors were not co-axial. Often broader linewidths or lower signal intensities prevent the observation of ^{53}Cr hyperfine structure from samples containing Cr isotopes in natural abundance. In such situations, it is usually necessary to work with isotopically-enriched materials if the maximum information is to be obtained from EPR spectra; this is analogous to the use of the ^{55}Mo isotope to positively identify Mo(III) and Mo(V) signals in EPR investigations of the reaction of Mo(VI) with humic acids [17].

The electronic structures of Cr(III) complexes are invariably high spin with three unpaired electrons [13], and the relative energies of the electronic transitions are strongly dependent on the molecular symmetry around the ion. In octahedral symmetry, spectra are isotropic with deviations from the free spin value being proportional to the magnitude of the ligand field splitting. Deviations from pure cubic symmetry, however, result in transitions that can occur over a wide range of energies, dependent in a major way on the magnitudes of the zero field splitting parameters, D and E [18]. The condition for pure cubic symmetry corresponds to $D = 0$, and there is a single transition as observed for the $Cr(H_2O)_6^{3+}$ ion [5]. However, with increasing D, multiple transitions occur, and samples in which Cr(III) is present with a range of values for D (and also E) (as could often occur with natural specimens) produce EPR spectra with broad lines (e.g. [19]).

4. Results and discussion

The EXAFS spectra of the product of the reaction of Cr(VI) with coir pith and Cr(III) sulfate are shown in Fig. 2 along with their Fourier transforms. The Cr–O interatomic distance of 1.95 ± 0.02 Å in the coir pith sample is typical of Cr(III), and indicates that after adsorption on coir pith, the chromium is coordinated to six oxygen atoms and most, if not all, is in the Cr(III) form. This result is similar to that obtained for the adsorption of Cr(VI) on hops biomass [14] and on brown seaweed [20].

The EPR spectra of Cr/coir pith before and after adsorption of Cr(VI) at pH 2 are shown in Fig. 3a and b. Although the blank sample contains a broad signal typical of that assigned to iron oxides (e.g. [21]), the sample with adsorbed Cr has a much larger absorption in this region. The spectrum of an equivalent sample prepared at pH 10 was also broad (not shown), though in this case a number of distinct features were present. Furthermore, the EPR spectrum of a freeze-dried sample of a Cr-rich waste water (Fig. 3c), in which there was a mixture of Cr(VI) and Cr(III) (P. Suksabye, unpublished results), is very similar to that of Fig. 3b. Thus, the broad feature in Fig. 3b almost certainly arises mainly from paramagnetic Cr species.

However, in addition to the broad peak described above, Fig. 3b also shows the presence of some weaker peaks, which are shown in expanded form in Fig. 4a. This latter spectrum is similar to that reported previously [5], although in the earlier paper the sloping
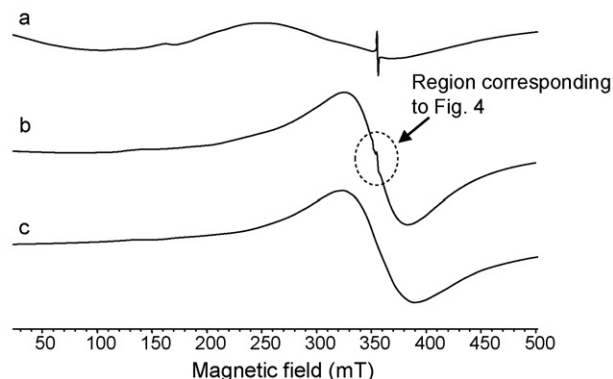

Fig. 3. 1st derivative EPR spectra at room temperature of dried powders of coir pith (a) before and (b) after reaction with Cr(VI) at pH 2, and (c) a dried sample of a Cr-rich wastewater. Spectra were recorded using 20 mW microwave power and 1.0 mT modulation amplitude.
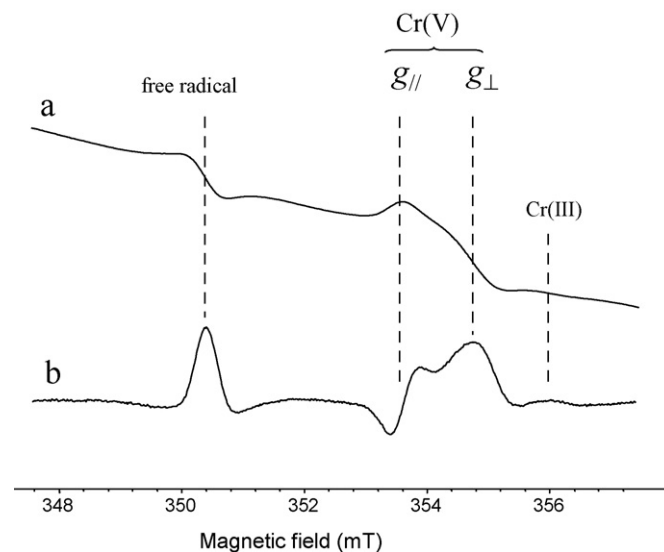

Fig. 4. EPR spectra at room temperature of the dried powder resulting from the adsorption of Cr(VI) on coir pith at pH 2, (a) 1st derivative and (b) 2nd derivative recording. Spectra were recorded using 20 mW microwave power and 0.5 mT modulation amplitude.

baseline was thought to correspond to the presence of an iron oxide phase and removed numerically in order to improve the appearance of the spectrum. The spectrum in Fig. 4a consists of three components that were previously assigned to free radical, Cr(V) and Cr(III) signals [5]. The same components were also observed with the sample prepared at pH 10 (data not shown), albeit with appreciably different relative intensities for the Cr-derived signals.

In an attempt to prove the assignments of the features in Fig. 4a to Cr(V) and Cr(III), similar measurements were made using chromium enriched in the ^{53}Cr isotope. However, instead of observing the expected ^{53}Cr hfs, the spectral components previously assigned to Cr(V) and Cr(III) disappeared. Presumably the much greater spectral width resulted in a decrease in amplitude to such an extent that the ^{53}Cr peaks were unobservable. Interestingly, the wide scan spectrum was very similar to that of Fig. 3b, as expected for the broad peak originating from chromium (note that the ^{53}Cr hfs would not be expected to be observed here because of the large overall width).

The broad EPR signal in Fig. 3b is not definitive for Cr(III), although it is consistent with that ion in a non-cubic environment. It could, for example, result from exchange interactions between any paramagnetic ions in close proximity to one another, and in environmental samples such a peak is usually assigned to iron oxides. The present measurements, however, show that it corresponds (largely) to Cr in the Cr/coir pith samples. The possibility of a Cr(V) contribution to the broad resonance in Fig. 3b cannot be excluded, especially if it precipitates on the surface of the coir pith, but it definitely does not correspond to Cr(V) in magnetically dilute (i.e. mononuclear complex) forms, since these would produce narrow lines as illustrated in Fig. 1.

In order to address the problem of whether the broad peak in Fig. 3b contains a major contribution from magnetically interacting Cr ions, additional adsorption measurements were performed using Cr/Al mixtures, in which the Al was present in up to 10-fold excess. The diamagnetic Al^{3+} ion would be expected to prevent (or at least inhibit) the formation of any Cr-rich domains on the coir pith surface. However, the resulting EPR spectra (not shown) were very similar to that of Fig. 3b, but with lower intensity. Thus, the major contribution to the intensity of this spectrum comes from magnetically dilute Cr species, which because of the large linewidth must be Cr(III), a result which is consistent with the observation of a similar spectrum with Cr(III)-rich wastewater. Consequently, both EXAFS and EPR results are consistent with one another, and both indicate that Cr(III) is the major form of chromium in coir pith after adsorption of Cr(VI).

EPR spectra are conventionally recorded as the 1st derivatives of the microwave absorption, with the result that the heights of narrow peaks are enhanced relative to those of broader peaks; this is further accentuated when 2nd derivative recordings are used to improve spectral resolution (e.g. Fig. 4b). It is possible, therefore, to completely miss the contribution from a broad component when optimizing the resolution of narrow features in a spectrum. Because of the wide range of paramagnetic entities that can be found in natural samples, it is recommended that EPR spectra should first of all be acquired using a wide scan range, similar to that used in Fig. 3. Then when the regions in which absorptions occur have been identified, they can be investigated in more detail using narrower field scans as was done for Fig. 4. However, even with careful experimentation it may be difficult to identify unambiguously the sources of all of the features in a single EPR spectrum. This problem is illustrated in the present paper for the broad $g = 2.0$ feature, where the assignment to Cr(III) was only possible after performing additional measurements using Cr/Al mixtures adsorbed on coir pith in order to exclude the formation of magnetically interacting Cr ion clusters. It should also be recognized that there may be large differences in linewidth and saturation characteristics between different spectral components (e.g. between free radicals and paramagnetic metal ions), with the result that there may be large differences in the values for the modulation amplitude and microwave power needed for optimizing their spectra. Thus quantitative measurements are difficult and generally require extensive spectral measurements involving a range of acquisition conditions, as well as reference to appropriate standard reference compounds. Caution should, therefore, be exercised when attempting to use EPR spectroscopy as a quantitative analytical tool.

5. Conclusions

The present measurements establish that chromium in coir pith that had been saturated with Cr(VI) is largely in the Cr(III) oxidation state. The discrepancy in the conclusions from previous measurements using EPR and XANES [2,3,5] has been shown to result from the choice of inappropriate parameters for acquiring the EPR spectra. As a result, the presence of a major Cr-rich phase, which produces a very broad signal, was not detected in the original EPR measurements. In order to avoid such problems, it is recommended that all EPR investigations of natural samples include spectra recorded over a wide scan range prior to conducting measurements over specific areas of interest.

References

[1] H. Parab, S. Joshi, N. Shenoy, R. Verma, A. Lali, M. Sudersanan, Uranium removal from aqueous solution by coir pith: equilibrium and kinetic studies, Bioresour. Technol. 96 (2005) 1241–1248.

[2] P. Suksabye, P. Thiravetyan, W. Nakbanpote, S. Chayabutra, Chromium removal from electroplating wastewater by coir pith, J. Hazard. Mater. 141 (2007) 637–644.

[3] P. Suksabye, P. Thiravetyan, W. Nakbanpote, Column study of chromium(VI) adsorption from electroplating industry by coconut coir pith, J. Hazard. Mater. 160 (2008) 56–62.

[4] A. Ewecharoen, P. Thiravetyan, W. Nakbanpote, Comparison of nickel adsorption from electroplating rinse water by coir pith and modified coir pith, Chem. Eng. J. 137 (2008) 181–188.

[5] P. Suksabye, A. Nakajima, P. Thiravetyan, Y. Baba, W. Nakbanpote, Mechanism of Cr(VI) adsorption by coir pith studied by ESR and adsorption kinetics, J. Hazard. Mater. 161 (2009) 1103–1108.

[6] C. Namasivayam, D. Sangeetha, Removal of molybdate from water by adsorption onto $ZnCl_2$ activated coir pith carbon, Bioresour. Technol. 97 (2006) 1194–1200.

[7] C. Namasivayam, D. Sangeetha, Removal and recovery of vanadium(V) by adsorption onto $ZnCl_2$ activated carbon: kinetics and isotherms, Adsorption 12 (2006) 103–117.

[8] D. Kavitha, C. Namasivayam, Experimental and kinetic studies on methylene blue adsorption by coir pith carbon, Bioresour. Technol. 98 (2007) 14–21.

[9] H. Parab, S. Joshi, N. Shenoy, A. Lal, U.S. Sarma, M. Sudersanan, Esterified coir pith as an adsorbent for the removal of Co(II) from aqueous solution, Bioresour. Technol. 99 (2008) 2083–2086.

[10] B. Ravel, M. Newville, *ATHENA, ARTEMIS, HEPHAESTUS*: data analysis for X-ray absorption spectroscopy using *IFEFFIT*, J. Synchrotron Rad. 12 (2005) 537–541.

[11] M. Newville, P. Livins, Y. Yacoby, E.A. Stern, J.J. Rehr, Near-edge x-ray-absorption fine structure of Pb: a comparison of theory and experiment, Phys. Rev. B47 (1993) 14126–14131.

[12] N. Binsted, EXCURV98, European Synchrotron Radiation Facility, Grenoble, France, 1998.

[13] F.A. Cotton, G. Wilkinson, C.A. Murillo, M. Bochmann, Advanced Inorganic Chemistry, Wiley-VCH, Weinheim, Germany, 1999.

[14] J.G. Parsons, M. Hejazi, K.J. Tiemann, J. Henning, J.L. Gardea-Torresdey, An XAS study of the binding of copper(II), zinc(II), chromium(III) and chromium(VI) to hops biomass, Microchem. J. 71 (2002) 211–219.

[15] J.L. Gardea-Torresdey, K.J. Tiemann, V. Armendariz, L. Bess-Oberto, R.R. Chianelli, J. Rios, J.G. Parsons, G. Gamez, Characterization of Cr(VI) binding and reduction to Cr(III) by the agricultural byproducts of *Avena monida* (oat) biomass, J. Hazard. Mater. 80 (2000) 175–188.

[16] B.A. Goodman, J.B. Raynor, Electron spin resonance of transition metal complexes, Adv. Inorg. Chem. Radiochem. 13 (1970) 135–362.

[17] B.A. Goodman, M.V. Cheshire, Reduction of molybdate by soil organic matter. EPR evidence for formation of both Mo(V) and Mo(III), Nature 299 (1982) 618–620.

[18] F.E. Mabbs, D. Collison, Electron Paramagnetic Resonance of d Transition Metal Compounds, Elsevier, Amsterdam, 1992.

[19] A. Levina, R. Codd, C.T. Dillon, P.A. Lay, Chromium in biology: toxicology and nutritional aspects, Prog. Inorg. Chem. 51 (2002) 145–250.

[20] D. Park, Y.-S. Yun, J.M. Park, XAS and XPS studies on chromium-binding groups of biomaterial during Cr(VI) biosorption, J. Colloid Interface Sci. 317 (2008) 54–56.

[21] B.A. Goodman, P.L. Hall, Electron paramagnetic resonance spectroscopy, in: M.J. Wilson (Ed.), Clay Mineralogy: Physical Determinative Methods, Chapman & Hall, London, 1994, pp. 173–225.